

Starbursts In Ultraluminous Infrared Galaxies - Fueling And Properties

Paul P. van der Werf

Leiden Observatory, P.O. Box 9513,
NL 2300 RA Leiden, The Netherlands

Abstract. The properties of starbursts in ultraluminous infrared galaxies are discussed, with particular emphasis on the fueling, the amount of extinction and the intrinsic properties of the nuclear starbursts. It is shown by the example of NGC 6240 that the H_2 vibrational lines can be used to measure the rate of gas inflow into the potential well, which is sufficient to fuel a nuclear starburst of the intensity required to account for the far-infrared emission. It is shown that in Arp 220 the faintness of all tracers of ionized gas can be accounted for by Lyman continuum absorption by dust within the ionized regions, combined with significant (but not extreme) extinction; there is no reason to invoke the presence of extreme extinction, an old starburst, or an additional non-stellar power source in Arp 220.

1 Introduction

Are ultraluminous infrared galaxies (ULIGs) powered by intense bursts of star formation or is an additional source of energy, such as an active galactic nucleus (AGN) required? In order to address this question, it is instructive to compare the near-infrared spectra of ULIGs and lower luminosity starburst galaxies. In starburst galaxies of low or moderate luminosity, the dominant emission line is the $Br\gamma$ line, underlining the importance of massive young stars in the energetics of these objects. The brightest H_2 rovibrational line, the $H_2 v = 1 \rightarrow 0 S(1)$ line, is typically fainter [7,8,10,11,21,20]. In contrast, in ULIGs the $H_2 v = 1 \rightarrow 0 S(1)$ line is significantly brighter than the $Br\gamma$ line, which is often not even detected [5,9]. This behaviour shows that ULIGs are not just scaled-up starburst galaxies. An extreme case of is presented by NGC 6240 (Fig. 1), where the $H_2 v = 1 \rightarrow 0 S(1)$ line is 40 times brighter than $Br\gamma$. The low ratio of $Br\gamma$ luminosity to FIR luminosity in ULIGs has been used to argue against star formation as the power source of ULIGs, for instance in the nearby ULIG Arp 220, where a starburst with the low $Br\gamma$ luminosity observed can account for at most 10% of the bolometric luminosity of the galaxy [1,12]. However, spectroscopy of ULIGs at longer wavelengths with the Infrared Space Observatory (ISO) revealed bright emission lines from powerful starbursts, which are the dominant power source

to appear in “Starburst galaxies: near and far”, eds. D. Lutz & L. J. Tacconi, (Springer)

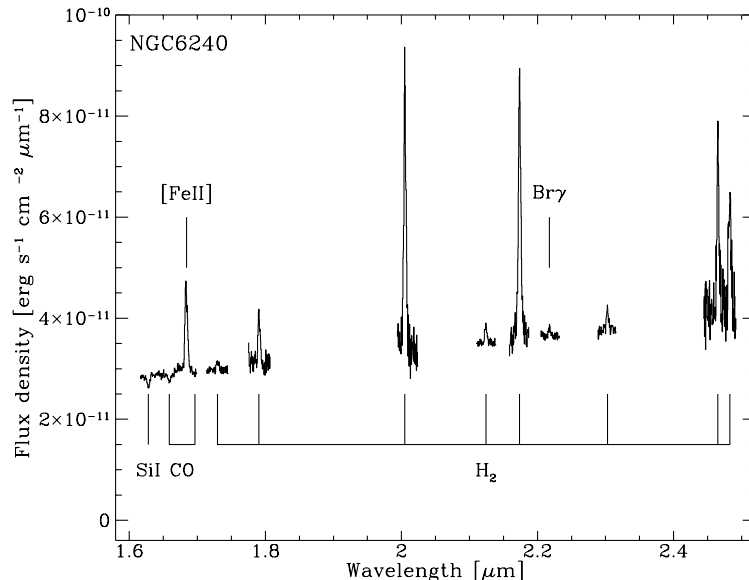


Fig. 1. Spectra of NGC 6240 in selected parts of the near-infrared H and K bands, integrated over a $4'' \times 4''$ region [19]

in most of the objects studied, but are obscured at shorter wavelengths [4]. Motivated by these results, in this paper the physical processes revealed by the K -band spectra of ULIGs are reexamined in the context of the starburst scenario. In Sect. 2 the origin of the H_2 line emission is discussed, while Sect. 3 addresses the faintness of $Br\gamma$.

2 Origin of the H_2 emission in ULIGs

The most extreme vibrational H_2 emission is found in the nearby luminous merger NGC 6240: $7 \cdot 10^7 L_\odot$ is emitted in the $H_2 v = 1 \rightarrow 0$ S(1) line alone (for $H_0 = 75 \text{ km s}^{-1} \text{ Mpc}^{-1}$ and with no correction for extinction). This line contains 0.012% of the bolometric luminosity of NGC 6240, which is considerably higher than any other galaxy [18]. Together the vibrational lines may account for 0.1% of the total bolometric luminosity.

Imaging of the $H_2 v = 1 \rightarrow 0$ S(1) emission from NGC 6240 has shown that the H_2 emission peaks *between* the two remnant nuclei of the merging system [18]. This morphology provides a unique constraint on the excitation mechanism, since it argues against any scenario where the excitation is dominated by the stellar component (e.g., UV-pumping, excitation by shocks or X-rays from supernova remnants). Instead, the favoured excitation mechanism is slow shocks in the nuclear gas component, which, as shown by high resolution interferometry in the CO $J = 2 \rightarrow 1$ line [15], also peaks between the nuclei of NGC 6240.

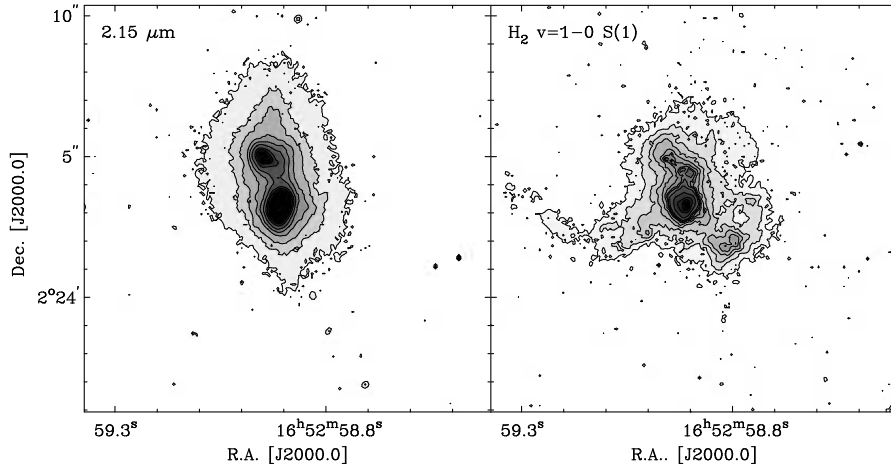


Fig. 2. High resolution imaging of NGC 6240 in the $\text{H}_2 v = 1 \rightarrow 0 \text{ S}(1)$ line and the $2.15 \mu\text{m}$ continuum with NICMOS/HST [19]

What is the role of these shocks? In the shocks mechanical energy is dissipated and radiated away, mostly in spectral lines (principally H_2 , CO , H_2O and $[\text{O I}]$ lines). This energy is radiated away at the expense of the orbital energy of the molecular clouds in the central potential well. Consequently, the dissipation of mechanical energy by the shocks will give rise to an infall of molecular gas to the centre of the potential well. Therefore, *the H_2 vibrational lines measure the rate of infall of molecular gas into the central potential well.* This conclusion can be quantified by writing

$$L_{\text{rad}} = L_{\text{dis}}, \quad (1)$$

where L_{rad} is the total luminosity radiated by the shocks and L_{dis} the dissipation rate of mechanical energy, giving rise to a molecular gas infall rate \dot{M}_{H_2} given by

$$L_{\text{dis}} = \frac{1}{2} \dot{M}_{\text{H}_2} v^2, \quad (2)$$

where v is the circular orbital velocity at the position where the shock occurs.

Using a K -band extinction of $0^{\text{m}}15$ [18], the total luminosity of H_2 vibrational lines from NGC 6240 becomes $7.2 \cdot 10^8 L_{\odot}$; inclusion of the purely rotational lines observed with ISO approximately doubles this number, so that $L_{\text{rad}} = 1.5 \cdot 10^9 L_{\odot}$.

In order to use this number to estimate \dot{M}_{H_2} , it is necessary to establish more accurately the fraction of the H_2 emission that is due to infalling gas. Observations with NICMOS on the Hubble Space Telescope (HST) provide the required information (Fig. 2) [19]. The NICMOS image shows that the emission consists of a number of tails (presumably related to the superwind also observed in $\text{H}\alpha$ emission), and concentrations associated with the two nuclei, and a further concentration approximately (but not precisely) between the two nuclei. The relative

brightness of the H_2 emission from the southern nucleus is deceptive, since this nucleus is much better centred in the filter that was used for these observations than the other emission components, in particular the northern nucleus. Taking this effect into account, it is found that 32% of the total H_2 flux is associated with the southern nucleus, 16% is associated with the northern nucleus, and 12% with the component between the two nuclei, the remaining 40% being associated with extended emission. Using inclination-corrected circular velocities of 270 and 360 km s^{-1} for the southern and northern nucleus respectively [16], and of 280 km s^{-1} for the central component [15], the mass infall rates derived using (1)–(2) are 80 $M_\odot \text{ yr}^{-1}$ for the southern nucleus, 22 $M_\odot \text{ yr}^{-1}$ for the northern nucleus and 28 $M_\odot \text{ yr}^{-1}$ for the central component.

The derived molecular gas inflow rate to the two nuclei is remarkably close to the mass consumption rate by star formation of approximately 60 $M_\odot \text{ yr}^{-1}$, indicating that the H_2 emission from the nuclei directly measures the fueling of the starbursts in these regions. This analysis shows that the central regions of NGC 6240 are being fueled at a rate sufficient to maintain starburst activity at the level required to account for the FIR luminosity.

3 Dusty, compact starbursts in ULIGs

Accepting the starburst model, the faintness of $\text{Br}\gamma$ and other recombination lines remains to be addressed. As pointed out in Sect. 1, it is evident that selective extinction towards the regions of most recent massive star formation plays a significant role in suppressing the $\text{Br}\gamma$ emission. Can this effect be quantified?

The nearby ULIG Arp 220 has been studied in detail with the ISO satellite. Based on an upper limit on the ratio of the $[\text{S III}]$ 18 and 33 μm lines, and a high $\text{Br}\alpha$ over $\text{Br}\gamma$ flux ratio, an extinction $A_V = 50 \pm 10^m$, located purely in an absorbing foreground screen was proposed [14]. However, the supporting arguments have now weakened significantly. In the first place, a better understanding of the calibration of the $[\text{S III}]$ 33 μm spectrum has made the upper limit on the $[\text{S III}]$ 18 to 33 μm flux ratio less strict by approximately a factor of two [4]. Secondly, the $\text{Br}\alpha$ flux from ISO [14] is almost certainly an overestimate: the $\text{Br}\alpha$ line displays, on top of a highly structured baseline, a double-peaked structure, which is absent in any other line (including long-wavelength lines such as the well-detected $[\text{S III}]$ 33 μm line). The velocity difference between the two peaks in $\text{Br}\alpha$ is approximately 600 km s^{-1} and therefore cannot be attributed to motion of the two nuclei of Arp 220, which have a radial velocity difference of approximately 200 km s^{-1} [12]. The same velocity difference of 200 km s^{-1} is found in long-slit $\text{Br}\gamma$ spectra of the Arp 220 nuclei [6]. An integrated high-resolution $\text{Br}\gamma$ spectrum (Fig. 3) shows no trace of a double-peaked structure, indicating that the high $\text{Br}\alpha$ flux found with ISO is most likely dominated by structure in the spectral baseline. The extinction derived from the $\text{Br}\alpha/\text{Br}\gamma$ ratio should thus be used as an upper limit. A further argument against an obscuring foreground screen with $A_V \approx 50^m$ is furnished by the derived Lyman continuum fluxes, which increase as shorter wavelength tracers are used [4], a behaviour sug-

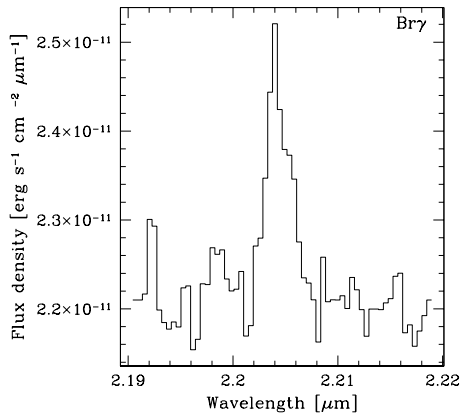


Fig. 3. Integrated spectrum of Br γ emission from Arp 220 [17]

gesting that the extinction has been overestimated. Finally, a strong limit on the presence of an intense, highly obscured, but otherwise normal starburst follows from the upper limit to the free-free emission at millimetre wavelengths [12]. These results indicate that either a foreground screen with a lower visual extinction, or a model with mixed emission and absorption needs to be adopted.

This result does however *not* imply the presence of a strongly aged starburst, or an additional source of power in Arp 220, since the preceding analysis ignored the role of Lyman continuum absorption by dust within the ionized regions. If most of the ionizing radiation is absorbed by dust grains rather than hydrogen atoms, a dust-bounded (rather than hydrogen-bounded) nebula results, and all tracers of ionized gas (recombination lines, fine-structure lines, free-free emission) will be suppressed. If the H II regions in Arp 220 are principally dust-bounded, the observational properties of Arp 220 can be accounted for, even with only moderate extinction. Since the dust would also absorb far-ultraviolet radiation longwards of the Lyman limit, the formation of photon-dominated regions would also be suppressed, and the thus the same mechanism can account for the faintness of the 158 μm [C II] line in Arp 220 and other ULIGs [3].

Is the Arp 220 starburst dominated by dust-bounded H II regions? The *average* molecular gas density in the $\sim 10^{10} M_{\odot}$ nuclear molecular complex in Arp 220 is $n_{\text{H}_2} \sim 2 \cdot 10^4 \text{ cm}^{-3}$ [12]. The strong emission from high dipole moment molecules such as CS, HCO⁺ and HCN argues for even higher densities: $\sim 10^{10} M_{\odot}$ of molecular gas (i.e., *all* of the gas in the nuclear complex) has a density $n_{\text{H}_2} \sim 10^5 \text{ cm}^{-3}$ [13]. At such densities the ionized nebulae created by hot stars are *compact* or *ultracompact* H II regions, where 50 to 99% of the Lyman continuum is absorbed by dust [22]. Observationally, hydrogen-bounded and dust-bounded H II regions can be distinguished by the quantity $R = L_{\text{FIR}}/L_{\text{Br}\gamma}$: for a wide range of parameters, $R < 3570$ implies that the nebula is hydrogen-

bounded, while $R > 35700$ implies that the nebula is dust-bounded [2]. For Arp 220, the $\text{Br}\gamma$ luminosity of $1.3 \cdot 10^6 L_{\odot}$ (from the spectrum in Fig. 3, with a distance of 77 Mpc) implies $R = 1.6 \cdot 10^5$ assuming an obscuring foreground screen with $A_V = 20^m$ (a model consistent with the results discussed above). Even with a foreground extinction of $A_V = 50^m$ (which is most likely an overestimate, as discussed above), a ratio $R = 1 \cdot 10^4$ would result, so that even in that case the absorption of Lyman continuum radiation by dust would play a significant role. The star formation takes place in (ultra)compact H II regions, where all of the usual tracers of ionized gas (recombination lines, fine-structure lines, free-free emission) are *quenched*, not extinguished. While this result significantly complicates the interpretation of diagnostics of massive star formation in ULIGs, it is safe to conclude that the properties of Arp 220 can be accounted for by an intense, and significantly (but not extremely) obscured starburst. There is no reason to invoke the presence of extreme extinction, a strongly aged starburst, or an additional power source in Arp 220.

References

1. L. Armus, D.L. Shupe, K. Matthews, B.T. Soifer, G. Neugebauer: ApJ **440**, 200 (1995)
2. M. Bottorff, J. Lamothe, E. Momjian, E. Verner, D. Vinković, G. Ferland: PASP **110**, 1040 (1998)
3. J. Fischer et al.: ‘An LWS spectroscopic survey of infrared bright galaxies’. In: *The universe as seen by ISO*, ed. P. Cox, M.F. Kessler (ESA SP-427, ESA Publications Division, Noordwijk, 1999) pp. 817–820
4. R. Genzel et al.: ApJ **498**, 579 (1998)
5. J.D. Goldader, R.D. Joseph, R. Doyon, D.B. Sanders: ApJ **444**, 97 (1995)
6. J.E. Larkin, L. Armus, R.A. Knop, K. Matthews, B.T. Soifer: ApJ **452**, 599 (1995)
7. A.F.M. Moorwood, E. Oliva: A&A **203**, 278 (1988)
8. A.F.M. Moorwood, E. Oliva: A&A **239**, 78 (1990)
9. T.W. Murphy, B.T. Soifer, K. Matthews, L. Armus, J.R. Kiger: AJ **121**, 97 (2001)
10. P.J. Puxley, T.G. Hawarden, C.M. Mountain: MNRAS **234**, 29P (1988)
11. P.J. Puxley, T.G. Hawarden, C.M. Mountain: ApJ **364**, 77 (1990); erratum ApJ **372**, 73 (1991)
12. N.Z. Scoville, M.S. Yun, P.M. Bryant: ApJ **484**, 702 (1997)
13. P.M. Solomon, S.J.E. Radford, D. Downes: ApJ **348**, L53 (1990)
14. E. Sturm et al.: A&A **315**, L133 (1996)
15. L.J. Tacconi, R. Genzel, M. Tecza, J.F. Gallimore, D. Downes, N.Z. Scoville: ApJ **524**, 732 (1999)
16. M. Tecza, R. Genzel, L.J. Tacconi, S. Anders, L.E. Tacconi-Garman, N. Thatte: ApJ **537**, 178 (2000)
17. P.P. van der Werf, F.P. Israel: in preparation (2001)
18. P.P. van der Werf, R. Genzel, A. Krabbe, M. Blietz, D. Lutz, S. Drapatz, M.J. Ward, D.A. Forbes: ApJ **405**, 522 (1993)
19. P.P. van der Werf, A.F.M. Moorwood, F.P. Israel: in preparation (2001)
20. L. Vanzi, G.H. Rieke: ApJ **479**, 694 (1997)
21. L. Vanzi, G.H. Rieke, C.L. Martin, J.C. Shields: ApJ **466**, 150 (1996)
22. D.O.S. Wood, E. Churchwell: ApJS **69**, 831 (1989)